EVALUATION OF MAGNETO RAYLEIGH-TAYLOR MODE GROWTH USING COMPARISONS OF 2D CALCULATIONS WITH RADIOGRAPHIC DATA

W. L. Atchison, R. J. Faehl, R. E. Reinovsky
Plasma Applications Group and Pulsed Power Program Office,
Los Alamos National Laboratory, Los Alamos, New Mexico 87545

Experiments being conducted at the Los Alamos National Laboratory Pegasus facility are examining stability issues for driving an aluminum liner with a pulsed magnetic field. The Pegasus facility provides a current of 5 to 8 Megamperes to compress a cylindrical liner. Liners of various size and thickness are used, depending on the specific experimental objectives. In several of these experiments, the outer surface clearly develops perturbations in the mass distribution. These perturbations are strongest when the aluminum is suspected to have melted and in some cases partially vaporized. A series of specific experiments was designed to examine the growth rate of these instabilities. These experiments involved machining a sine wave onto the outer surface of the liner to seed a given wavelength. Two-dimensional MHD calculations, using the measured current profile, were performed to model the behavior of the liner under magnetic field compression. These predictions were made with a 2D Eulerian code complete with a Steinberg-Guinan strength model. The results of these calculations will be discussed in this paper. The density contours at specific times will be compared with the processed radiography.

Introduction

Many applications of electromagnetic solid liner implosions require that the state of the liner in late time is smooth, intact, and predictable. A major concern is the unstable growth of initial perturbations during the implosion arising possibly from ordinary processes such as fabrication imperfections or irregularities. In fluids, the unstable growth of perturbations associated with the acceleration of a less dense fluid by a denser one is known as Rayleigh-Taylor instability. When the role of the lighter fluid is assumed by magnetic pressure, the term Magneto Rayleigh-Taylor instability[1, 2] is used. In both cases, the instability has been examined exhaustively. We are interested in a somewhat different situation here. A magnetic field still provides the driving force to accelerate the liner, but the liner itself is not in general a fluid. Instead, we have studied solid liners, which retain strength in an elastic-plastic state for much of the duration of the implosion. Sinusoidal perturbations have been machined into the outer surface of the liner to seed any unstable behavior. We have observed instability growth in PEGASUS-II experiments and found good agreement between the data and 2D MHD calculations. The growth and nonlinear phases exhibit dynamics somewhat different than classical Rayleigh-Taylor instability. The latter phase is particularly unique, evolving into coherent, disk-like structures at the same scale-length as the initial perturbations.

The topic of solid liner/plate instability has been addressed both experimentally[3-4] and theoretically[5-7]. Earlier experiments conducted by Barnes, etal.[3-4] were generically similar to the present ones, except that explosives provided the acceleration in those studies. They observed the expected growth behavior, but also found wavelength and amplitude dependent thresholds. These thresholds were correlated with simple theories, which included both yield strength and shear modulus. More sophisticated analysis of solid liner acceleration instabilities by Robinson and Swegle[6-7] provided a more detailed treatment of the processes, but did not generate any new data.

In this paper, we present the results of a series of pulsed power experiments, designed to investigate the quantitative evolution of unstable solid liners. A key diagnostic on these

0-7803-4214-3/97/$10.00 © 1997 IEEE

Report Documentation Page

Form Approved
OMB No. 0704-0188

1. REPORT DATE	2. REPORT TYPE	3. DATES COVERED
JUN 1997	**N/A**	**-**

4. TITLE AND SUBTITLE
Evaluation Of Magneto Rayleigh-Taylor Mode Growth Using Comparisons Of 2d Calculations With Radiographic Data

5a. CONTRACT NUMBER
5b. GRANT NUMBER
5c. PROGRAM ELEMENT NUMBER

6. AUTHOR(S)

5d. PROJECT NUMBER
5e. TASK NUMBER
5f. WORK UNIT NUMBER

7. PERFORMING ORGANIZATION NAME(S) AND ADDRESS(ES)
Plasma Applications Group and Pulsed Power Program Office, Los Alamos National Laboratory, Los Alamos, New Mexico 87545

8. PERFORMING ORGANIZATION REPORT NUMBER

9. SPONSORING/MONITORING AGENCY NAME(S) AND ADDRESS(ES)

10. SPONSOR/MONITOR'S ACRONYM(S)
11. SPONSOR/MONITOR'S REPORT NUMBER(S)

12. DISTRIBUTION/AVAILABILITY STATEMENT
Approved for public release, distribution unlimited

13. SUPPLEMENTARY NOTES
See also ADM002371. 2013 IEEE Pulsed Power Conference, Digest of Technical Papers 1976-2013, and Abstracts of the 2013 IEEE International Conference on Plasma Science. Held in San Francisco, CA on 16-21 June 2013. U.S. Government or Federal Purpose Rights License.

14. ABSTRACT
Experiments being conducted at the Los Alamos National Laboratory Pegasus facility are examining stability issues for driving an aluminum liner with a pulsed magnetic field. The Pegasus facility provides a current of 5 to 8 Megamperes to compress a cylindrical liner. Liners of various size and thickness are used, depending on the specific experimental objectives. In several of these experiments, the outer surface clearly develops perturbations in the mass distribution. These perturbations are strongest when the aluminum is suspected to have melted and in some cases partially vaporized. A series of specific experiments was designed to examine the growth rate of these instabilities. These experiments involved machining a sine wave onto the outer surface of the liner to seed a given wavelength. Two-dimensional MHD calculations, using the measured current profile, were performed to model the behavior of the liner under magnetic field compression. These predictions were made with a 2D Eulerian code complete with a Steinberg-Guinan strength model. The results of these calculations will be discussed in this paper. The density contours at specific times will be compared with the processed radiography.

15. SUBJECT TERMS

16. SECURITY CLASSIFICATION OF:			17. LIMITATION OF ABSTRACT	18. NUMBER OF PAGES	19a. NAME OF RESPONSIBLE PERSON
a. REPORT	b. ABSTRACT	c. THIS PAGE			
unclassified	**unclassified**	**unclassified**	**SAR**	**6**	

experiments has been the radiography configuration. Details of this configuration are presented in another paper at this conference[8]. Up to three separate radiograms were obtained for each experiment. Generally, these were at three different times during the implosion, and viewed the liner from three different azimuths. The high quality of these radiograms has permitted quantitative analysis of the morphology of the liner and detailed correlation with two-dimensional (2D) MHD simulations of the process. In the next section of this paper, we present some of the most distinctive features of the data, as well as a description of experiments. Simulations of the experiments using 2D resistive MHD calculations are described in the following section. Comparisons with the data are drawn. Finally, we summarize our results to date and present a hypothesis for the dominant physics responsible for the dramatic evolution of this solid liner instability.

Experimental results for a series of solid liner experiments on PEGASUS-II

The present experiments were performed on the PEGASUS-II capacitor bank at LANL. For this series of experiments, the bank was typically charged to 40-45 kV. This resulted in peak currents of 5-6.5 MA to our imploding liner loads at 7.5-8.0 μs after the circuit was closed. The liner was fabricated from the aluminum alloy 1100-0. Its inner radius was 2.36 cm and it was 0.413 cm thick. A thin coating of gold (5-12 μm) was plated onto the inner surface of the liner to provide a radiographic marker. The electrodes or glide planes were made of copper and had a glide plane angle of 8°. An aluminum rod with a 1.0 cm OD was placed on the axis, connecting the two electrodes. This center conductor permitted the measurement of the time of electrical rupture and release of magnitude of flux to the inside the liner. A B-dot probe was inserted into the region outside the center conductor but inside the liner to measure this signature.

The outer surface of the liner was divided at the mid-plane into two regions. Each half along the z-axis had a different machined surface. Table 1 summarizes the parameters for the three experiments conducted to date. These liners imploded radially with drive currents between 4.6-6.4 MA.

Table 1. Liner Stability Experiments 4 through 6

Liner Configuration	Side 1		Side 2		Peak Current
	Amplitude	Wavelength	Amplitude	Wavelength	
LS – 4	Smooth	None	50.0 μ	2.00 mm	4.6 MA
LS – 5	25.0 μ	2.0 mm	25.0 μ	0.75 mm	6.3 MA
LS – 6	12.5 μ	2.0 mm	12.5 μ	0.50 mm	6.4 MA

The amplitudes in Table.1 refer to the amplitudes of the initial sine wave ripples. Later when we compare radiographic data to calculations, we generally use peak-to-peak as a measure of amplitude.

A series of three side-looking X-ray radiographs were obtained with pulsed X-ray sources. Each experiment used three sources, which were placed at different azimuths around the liner chamber and fired at three different times. The radiographs were processed with a 5 pixel square median filter. The size of this filter at the film plane matches the blur width due to the x-ray source size. This minimizes the impact of film and digitizer noise. This data was further processed with an approximate discrete Abel inversion technique to produce attenuation factor contours in r and z. This process assumed an average linear attenuation coefficient with no spectral dependence on thickness of the absorber, no x-ray scatter, and azimuthal symmetry. A

two-dimensional reconstruction of the density distribution resulted, from which the shape of both the inner and outer surfaces was obtained. While the resulting contours are relatively imprecise, the results are sufficient to reconstruct the cross-sectional shape of the liner based on the radiograms.

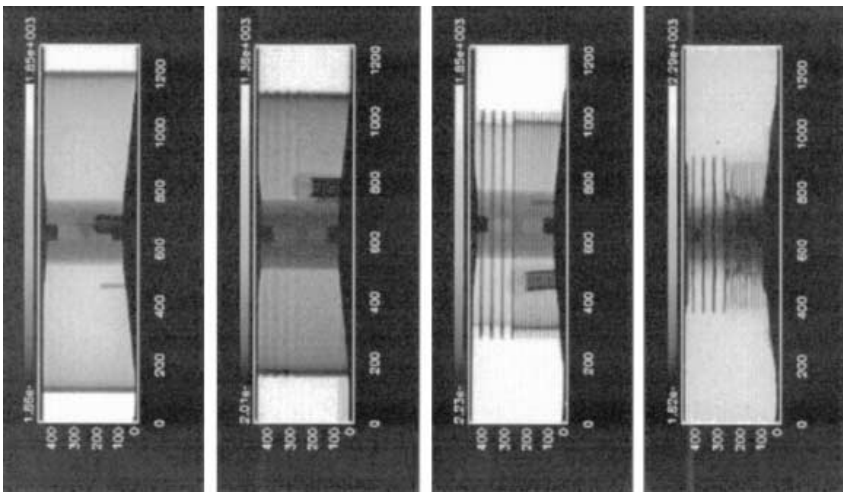

t = 0.00 μsec t = 6.50 μsec t = 7.50 μsec t = 9.50 μsec

Figure 1. LS-5 Radiogram

Figure 1 shows a typical sequence of radiographs, including the pre-shot static image (t = 0.00 μsec), for the LS-5 experiment. The wavelength on each side of the liner is clearly evident by t = 6.5 μs. By t = 8.0 μs, the 2.0 mm side has nearly "punched" through the bubble regions, and the 0.75 mm wavelength has also reached significant amplitudes. By t = 9.5 μs, both wavelengths have evolved into a series of well-defined discs, retaining their initial scale lengths with little evidence of wide scale mode mixing. This is even more remarkable since the inner edges of the discs have already impacted the central measuring unit (CMU).

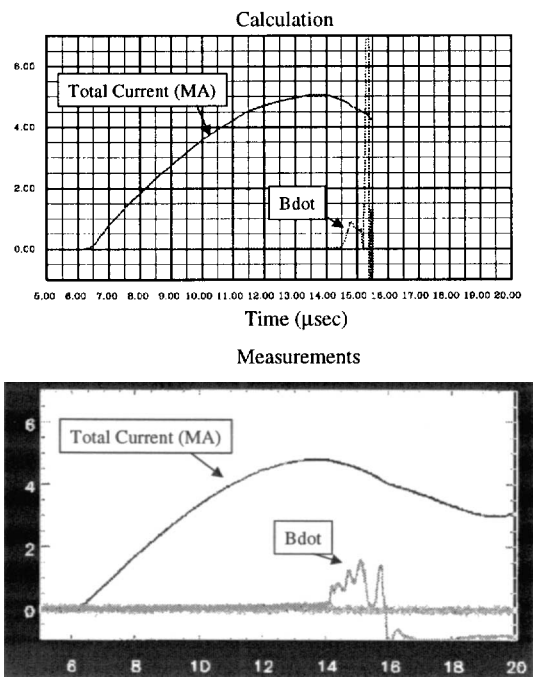

Figure 2. Current and B-dot Comparison

The radiographs show the mass distribution, but do not give direct information about the electrical condition of the liner. To infer such information, we placed a B-dot probe inside the liner, but external to the CMU. The onset of magnetic field into this interior region provides a clear signature of the electrical "rupture" of the liner. Figure 2 shows the measured B-dot signal for the LS-4 experiment, and the calculated B-dot signal for the same parameters. Both indicate that the onset of the magnetic field in the interior region was abrupt. They also suggest that no more than 40-50% of the field penetrates into the inner region. The bulk of the current is still carried by the liner material, even though much of the current path is relatively tenuous, hot plasma. Details of the calculation depend on accurate knowledge of the resistivity of the aluminum as it transitions from solid to liquid to plasma. The present knowledge of such resistivities is incomplete, especially in the strongly coupled plasma regime. However, the overall agreement is still very good.

2D MHD simulations of the experiments and comparison with data

2D resistive MHD calculations have been performed on configurations of LS-4, -5, -6. The measured current profile was used to drive the liner. Realistic dimensions, liner resistivity, and liner material properties were included in these calculations. Tabular equation of state data was used for the aluminum. The results were generally in startlingly good agreement with the data.

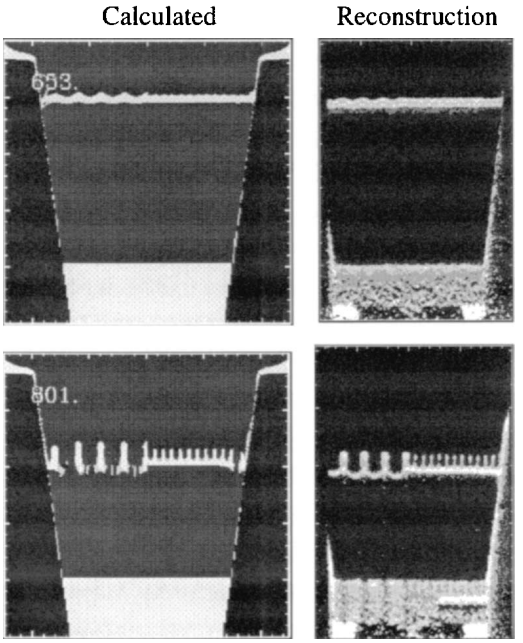

Figure 3. Code vs. Data Comparisons

Figure 3 shows a direct comparison between the calculated density distribution for LS-5 parameters on the 2.0 mm wavelength half of the liner at a time t = 8.0 μs, and the reconstructed density distribution obtained from the radiogram at the same time. The calculation appears to be approximately 0.2 μs faster than the experiment, but all of the essential features are present. The spike-and-bubble amplitude of the "outer" surface perturbation has grown to a level of roughly four times the initial liner thickness. The initial wavelength has remained the dominant scale length; there is virtually no evidence of mode mixing at this time. By late time in the instability growth, the surface shape has departed significantly from sinusoidal shape. The almost square wave structure seen in both radiographs and calculations would decompose into a broad Fourier spectrum, but this is an artifact of force fitting sinusoidal basis functions onto the shape. Even more dramatic agreement occurs at the time of last radiograph, t = 9.0 μs in LS-5. By this time, the imagery clearly shows that there is no significant mass left in the bubble regions. The spike regions moreover have been compressed into thick, narrow disc-like features. These discs show little if any evolution in shape once they have reached this state, even after the inner boundary has impacted onto the center conductor. These features are clearly seen in the calculations. A qualitative examination of the calculations indicates very little mass is expelled inward from the bubble regions. Instead, it appears to be axially transported into the discs.

Figure 3 is typical of the agreement we find between the data and the calculations on all three PEGASUS experiments in this series. A more quantitative description of the instability evolution can be obtained by plotting the calculated time history of the spike-and-bubble growth and comparing it with the measured amplitude. We show an example of this from LS-4 and LS-5 parameters in Figure 4. Figure 6 shows a comparison of the growth for the same initial amplitude but different perturbation wavelength. This clearly demonstrates that the long wavelength (2.0-mm) half begins growing significantly earlier than does the short wavelength (0.5 mm) side. However, late in time when the short wavelength begins to grow, its rate of growth is much faster. For these parameters, the long wavelength side is always dominant. There may be parameters, however, in which the short wavelengths can actually overtake the long wavelength ones, late in the pulse. We emphasize that neither the radiographs nor the calculations show evidence of spatial mixing between the two sides, so the late time growth on

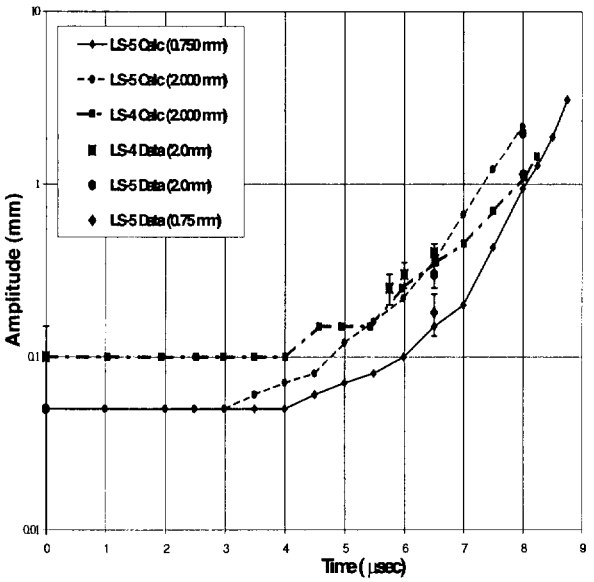

Figure 4. Data/Calculation Comparison

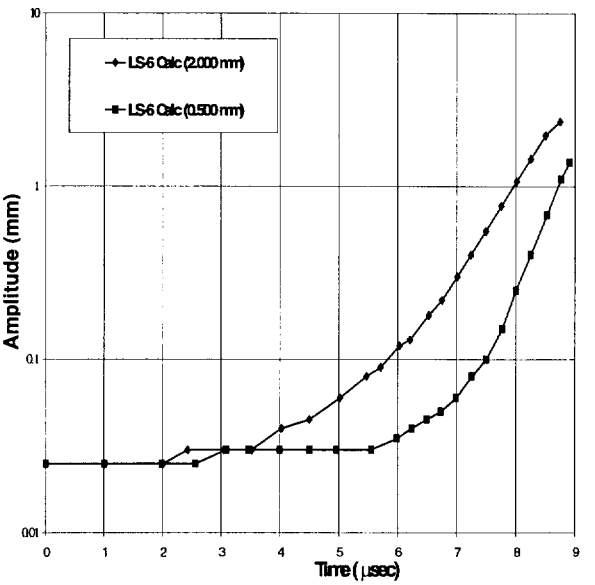

Figure 5. Growth Rate Comparison

the 0.5-mm side is probably independent of the amplitude of the longer wavelengths. Finally, the electrical properties of instability must be addressed. The magnetic probe placed near the center conductor always measures a sharp increase in current at or near the time in which the radiographs indicate that the bubbles have ruptured. The magnitude of the current flowing through the center conductor never exceeds 50% of the total current. Most of the current is still being conducted through the hot, tenuous regions between the discs. The calculations confirm this behavior. They further show that the discs are sufficiently resistive that the current flows through them, not around them.

Summary and conclusions

There are several significant conclusions that can be drawn from the series of experiments LS-4, LS-5, and LS-6 performed on the PEGASUS II capacitor bank. First, we have found that longer wavelengths begin to grow sooner, but that when the shorter wavelengths do begin to grow, they may grow faster. There appear to be several competing mechanisms present. There is strong computational evidence that heterogeneous resistivity profiles, caused by additional heating due to non-uniform diffusion, enhances melt preferentially in bubble region. On the other hand, spikes still retain strength at time of rupture. There is certainly competition between magnetic diffusion, resistivity, and elastic-plastic flow. The last effect seems to be dominant at 2 mm; the other are more critical at 0.5-mm. Axial flow appears to be the strongest effect during liner rupture, and disc formation. We are still studying these processes to derive a more integrated model for the liner stability and continue to make progress.

References

1. Harris, E. G., "Rayleigh-Taylor Instabilities of a Collapsing Cylindrical Shell in a Magnetic Field, *Phys.Fluids,* **5,** 1057-1062, 1962.
2. Harris, E. G.W., and, Dienes, J.K., "Taylor Instability in a Viscous Fluid" *Phys. Fluids,* **9,** 2518-2519, 1966.
3. Barnes, J.F., Blewett, P.J., McQueen R.G., Meyer, K.A., and Venable, D., "Taylor Instability in Solids", *J. App. Phys.,* **45,** 727-732, 1974.
4. Barnes, J.F.

5. Drucker, D.C., *Mechanics Today,* **Volume 5, Oxford**, Pergamon, 1980, 37-47.
6. Lebedev, A.I., Nisovtsev, P.N., and, Rayevsky, V.A.,"Rayleigh-Taylor Instability in Solids", *The 4th International Workshop on the Physic of Compressible Turbulent Mixing,* Cambridge, England, 29 March - 1 April 1993.
7. Swegle, J.W., and, Robinson, A.C., "Acceleration Instability in elastic-plastic solids. I. Numerical simulations of plate acceleration", *Journal of Applied Physics,* **66,** 2838-2858, 1989; Robinson, A.C., and, Swegle, J.W., "Acceleration Instability in elastic-plastic solids. II. Analytic techniques", *J. Applied Physics,* **66,** 2859-2872, 1989.
8. King, N.S.P., D. Morgan, A.W.Obst, D. Platts, D.S. Sorenseon, "Performance of the Multi-Pulse X-Ray Imaging System for the Pulsed Power Hydrodynamic Experiments at LANL", Proc. 11th IEEE International Pulsed Power Conference. (1997).